INCUS as RainCube and TEMPEST-D Legacy

Simone Tanelli[1], Ziad. S. Haddad[1], Susan van den Heever[2], Shannon Brown[1], Steven C. Reising[2]

1 - Jet Propulsion Laboratory, California Institute of Technology
4800 Oak Grove Dr., Pasadena, CA 91109; 818-354-1100

2 - Department of Atmospheric Science,
Colorado State University, Fort Collins, CO 80523-1371

ABSTRACT

RainCube (**Ra**dar **in** a **Cube**Sat) and **TEMPEST-D** (Temporal Experiment for Storms and Tropical Systems - Demonstration) demonstrated in 2018 that deployment of active and passive microwave sensors to monitor storms and precipitation from space is possible on platforms as small as 6U CubeSats. Despite their implementation as high-risk technology demonstrations, with very low budgets compared to their predecessors, they both survived more than two years in orbit (well beyond their commitments). These demonstrations enabled meeting several long-standing unmet needs of the scientific and operational weather and climate communities. Among them is the necessity to observe the evolution of the vertical structure of convective storms in the Tropics at the temporal scales relevant to convective processes (i.e. tens of seconds to few minutes) in order to advance our understanding of convective processes and their representation in weather and climate models. The **INCUS** (Investigation of Convective Updrafts) mission concept aims at addressing this need by deploying 3 small satellites each carrying an augmented version of the RainCube radar. One of the 3 small satellites also includes a millimeter wave radiometer inherited from TEMPEST-D. In this presentation we illustrate some of the challenges, opportunities and achievements critical for the transition of the INCUS mission concept from being purely aspirational to viable in the span of a decade.

1 INTRODUCTION

The initial concept for the INCUS Mission was developed more than a decade ago in response to a long-standing need of the atmospheric sciences community to improve the temporal coverage by microwave instruments enough to resolve the evolution of storms at the convective time scale of minutes to tens of minutes. Pioneering missions such as TRMM (NASA/JAXA, Tropical Rainfall Measuring Mission [1]), CoudSat (NASA/CSA, [2,3]) and the A-Train, and GPM (NASA/JAXA, Global Precipitation Measurement mission [4]) demonstrated the high value of combined radar-radiometer measurements, however, given their deployment in Low Earth Orbit (LEO), they were also limited in their ability to observe any individual storm multiple times within its lifecycle. In particular, none of them could observe storms in any systematic way at the convective timescale (tens of seconds to tens of minutes). Therefore, the evolution of the processes driving the storm development (from genesis to growth to mature stage to dissipating) could not be observed around the global scale.

In broad strokes, three possible solutions exist to address this observational gap: (1) use of ground-based weather radars and other suborbital assets; (2) use of geostationary radars and radiometers; and (3) use of multiple radars and radiometers in train formation in LEO. The first is limited in terms of spatial coverage to industrially developed land masses and sporadic airborne or shipborne deployments. The second approach leads to the need for extremely large apertures given the distance from geostationary orbit. The third leads to the need for deployment of multiple copies of the same instrument. While each solution comes with its advantages and disadvantages, the third one had remained largely notional for more than a decade because of the cost of access to space and implementation of multiple units of science-grade instruments according to the classical reliability paradigms for space industry. This solution had remained realistically unaffordable for decades until the arrival of the SmallSat and CubeSat platforms, at which time the challenge moved to simultaneously miniaturizing, reducing cost, and preserving fundamental performance requirements for these types of radars. The RainCube and TEMPEST-D architectures were formulated exactly for this purpose, and their technology development advanced independently under a sequence of initiatives funded by either internal JPL Research and Development, NASA's Earth Science and Technology Office programs, or Small Business Innovation Research program. Eventually they both were selected independently to a 6U Cubesat technology demonstration in space (through ESTO's InVEST program for RainCube and through the Earth Venture Program for TEMPEST-D) and they were co-manifested for launch in June 2018. They proceeded to demonstrate their objectives by successfully operating for more than 2 years in LEO. The key lies in the simplification and miniaturization of the system architecture and of selected subsystems.

RainCube and TEMPEST-D have therefore opened-up a new realm of options for low-cost satellite platforms such as CubeSats, with obvious savings not only on the instrument implementation (especially beyond the first unit) but also the spacecraft and launch costs. We can now actually consider deploying a constellation of identical copies of the same instrument in various relative positions in LEO to address specific observational gaps left open by the current missions that require high-resolution vertical profiling capability. The importance of these measurements gaps has been addressed at several recent NASA workshops of the Weather Focus Area (April 2015) and the Atmospheric Composition, Chemistry, Dynamics and Radiation Focus Area (May 2014, e.g., "*One of the primary inhibitors in understanding how convective processes vary around the globe is the lack of time resolution in observations from space*." [5]).

The INCUS mission concept rests on two fundamental pillars : to leverage directly on the technology demonstrated by RainCube, TEMPEST-D (see Figure 1) and other small sat missions in order to deploy multiple spacecrafts within a budget traditionally realistic for the launch of a single copy of the science payload, and to combine the strengths of radar and radiometer observations in a

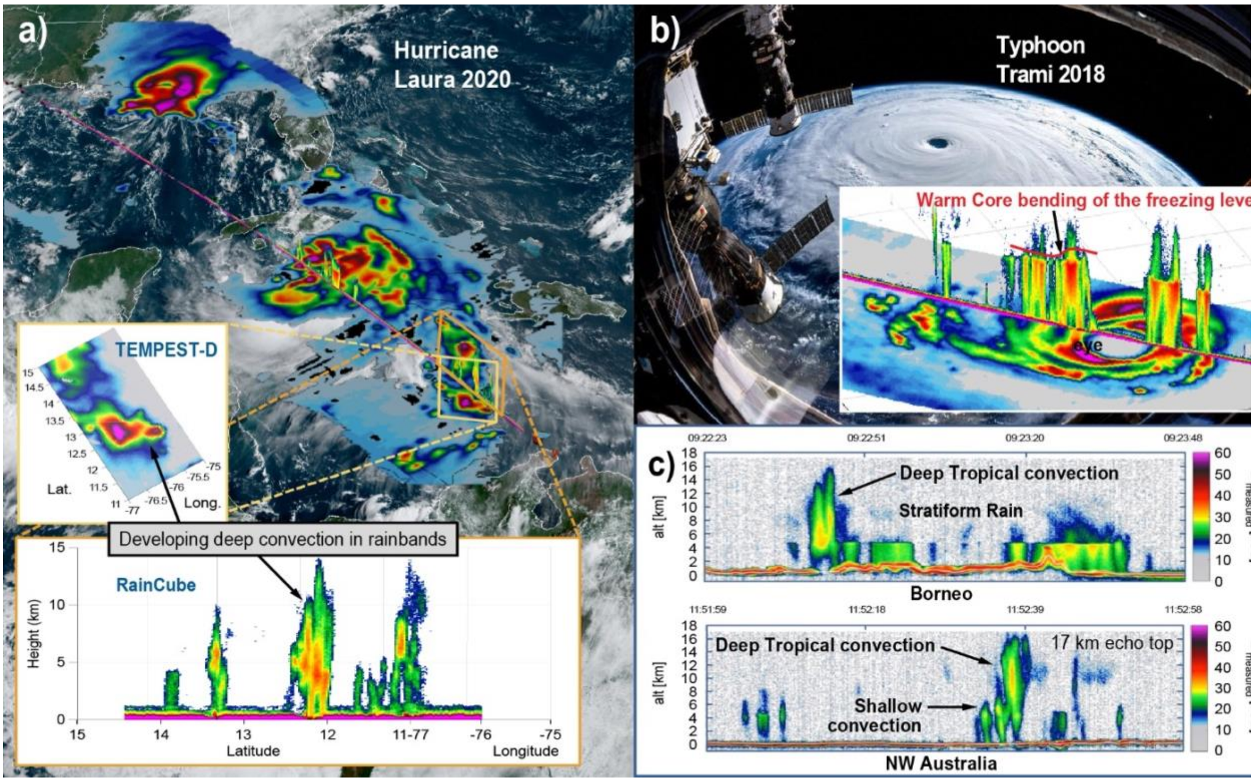

Figure 1. The success of RainCube and TEMPEST-D demonstrates the robustness of the INCUS Mission concept. a) RainCube's nadir curtain of precipitation reflectivity and TEMPEST-D swath of brightness temperature (only one channel shown) are shown overlaid to NOAA's Geostationary Operational Environmental Satellite East (GOES-E) imagery of Hurricane Laura and associated convective activity, zoomed in details are shown in the embedded panels; b) same as a) for Typhoon Trami; c) two examples of a mesoscale convective system (MCS) and deep tropical convection observed by RainCube at its native 8 km horizontal resolution. Instead of RainCube's 2-D curtain, DAR will sample a 3-D volume that is 15 km wide across track, with a ~3 km horizontal resolution.

targeted way to complement the Program Of Record and address a specific open question in weather and climate science: "Why do convective storms, heavy precipitation and clouds occur exactly when and where they do?" [6]. To achieve these, INCUS aims at capturing the rapid evolution of Convective Mass Flux profiles and storm structure on convective timescales throughout the tropics by deploying three copies of a Ka-band precipitation radar on three SmallSats spaced 30 and 90 seconds apart (i.e., total baseline from first to third is 120 seconds), so that the evolving vertical structure of condensate can be observed in that timescale. The three radars are complemented by a millimeter wave radiometer (deployed on one of the three spacecrafts) to provide essential observations of the atmospheric environment directly surrounding each observed storm.

2 THE INCUS MISSION CONCEPT

INCUS is composed of three small platforms in a train formation, separated by a few minutes in a precessing low Earth orbit (LEO). The orbit inclination will be finalized based on launch opportunities, with a preference for low inclination to maximize the sampling of storms in the tropics, although higher inclination precessing orbits are viable in achieving the objectives as shown in Table 1. Each of the three INCUS spacecrafts (Blue Canyon Technologies's X-SAT Venus) carries a Dynamic Atmospheric Radar (DAR) and one of them also carries also a Dynamic Millimeter-wave Radiometer (DMR).

All instruments are installed on the Integrated Payload Structure (IPS), which mates to the spacecraft (S/C). Figure 2 shows a notional mechanical configuration of the spacecraft that carries both a radar and a radiometer. Alternative mechanical configurations will be considered in the early phases of development as part of planned trade studies. Each of the subsystems finds its heritage in recent spaceborne missions (including technology demonstrations and commercial enterprises), and its ground data processing and algorithm development finds its heritage in more than 20 years of research, development and spaceborne mission experience of CIRA and the science team, respectively.

Science Objectives	Scientific Measurement Requirements		Instrument Function Requirements		Projected Performance (500 km altitude)	Mission Requirements (Top Level)
	Physical Parameters	Observables				
SCIENCE GOAL: To understand why, when, and where tropical convective storms form, and why only some storms produce extreme weather.						
BASELINE and THRESHOLD: **Science Objective 1:** (a) Determine how the environmental properties of CAPE, RH, temperature and vertical wind shear impact CMF in tropical convective storms as a function of storm type, lifecycle and diurnal cycle; and (b) evaluate these environment-CMF relationships in current CPMs, NWP models, and GCMs. **Science Objective 2:** (a) Determine the relationship between the CMF in tropical convective storms and the area and depth of the anvil clouds they produce, and (b) evaluate the corresponding CMF-anvil relationships in current CPMs and NWP models. **BASELINE ONLY:** **Science Objective 3:** (a) Determine the relationship between the CMF in tropical convective storms and the type and intensity of the weather they produce, and (b) evaluate the corresponding CMF-weather relationships in current CPMs and NWP models.	**5 to 19 km vertical profiles of:** 1. Condensed water mass (M) to ± 2 dB (~60% uncertainty in gm^{-3}) in each environmental state (Fig. D.2-4c) 2. Time rate of change of condensed water mass (M´) to ±1 dB min^{-1} 3. Condensate vertical velocity (W_C) to ±2 $m.s^{-1}$ (Fig. D.2-5a) 4. Fluxes of condensed water (Q_C) to ±0.5 $gm^{-2}s^{-1}$ (Figs. D.1-1b, D.2-5b)	**BASELINE:** Three nearly coincident vertical profiles of the radar reflectivity factor 30 sec, 90 sec, and 120 sec apart collected tropics-wide from tropical convective storms. **THRESHOLD:** Two nearly coincident vertical profiles of radar reflectivity factor 90 sec apart collected tropics-wide from tropical convective storms.	Radar Frequency	35.75 GHz ± 0.25 GHz	35.75 GHz ± 0.1 GHz	**Region & Time Sampling:** Mission Functional Requirements: Sampling 23.5°S to 23.5°N and all longitudes, precessing through the diurnal cycle Mission Design Requirements/ Constraints: Altitude within range of 450 km to 550 km. Inclination between 23.5° and 39°, with preferred science orbit inclination of 28.5° **Mission Duration:** 2 years with at least an 80% science collection duty cycle **Radar Footprints Overlap:** >80%, at least 90% of the time during science data collection **S/C Separation:** 3 S/C separated in time: S/C 1 to 2: 30 ± 10 sec; S/C 1 to 3: 120 ± 10 sec **Instrument Data Rate:** Up to 2.2 GByte per day per S/C **Minimum Downlink Frequency:** Weekly
			Sensitivity	≤17 dBZ	8 dBZ	
			Precision	≤1 dBZ	0.4 dBZ	
			Horizontal Resolution	≤3.5 km	3.1 km	
			Vertical Resolution	≤250m	240 m	
			Accuracy	≤2 dB	1.5 dB	
			Swath Width	≥11 km	15.5 km	
			Vertical Profile Window	At least 5–19 km	1 km below surface - 21 km above surface	
	5. Ice water path to within 200 gm^{-2} simultaneous with the radar observations	**BASELINE ONLY:** MM-wave radiances simultaneous with radar reflectivity profiles for tropical convective storms, tropics-wide.	Observation Center Frequencies	4 frequency channels between 150 and 190 GHz	165, 174, 178 and 181 ± 0.5 GHz	
			Horizontal Resolution	16 km for all 4 channels	16 km for all 4 channels	
			Swath Width	500 km	>1000 km	
			Accuracy	<5 K	<2K	
			Precision	<2 K	<1 K	
	Auxiliary Data Obtained from the PoR					
	Convective life-cycle index, RH, CAPE, wind shear, and temperature	3-D gridded analyses of water vapor, temperature, winds, and temperature from Global Modeling and Assimilation Office Modern-Era Retrospective Analysis for Research and Applications Version 2 (MERRA-2) [79] and ECMWF Reanalysis (ERA-5) [80]	Horizontal Resolution	0.5° × 0.5°	0.5° × 0.5°	
			Coincidence	Within 6 hr	3–6 hr	
	Ice water path to within 200 gm^{-2} at least 3 times over the storm lifecycle (initiation, mature, decay)	Global mm-wave radiances (from GPM, Advanced Microwave Sounding Unit B [AMSU-B], Microwave Temperature Sounder [MTS], ATMS)	Accuracy	5 K	<5 K	
			Horizontal Resolution	16 km	15 km	
			Temporal Resolution	120 min	<120 min	
	Convective anvil area, core size and spatial distribution of cores	Brightness temperature from geostationary IR [57, 78].	Horizontal Resolution	4km	4km	
			Coincidence	30 min	<30 min	
	Rainfall rates	Surface rainfall rates (mm/30 min) from Integrated Multi-satellitE Retrievals for GPM (IMERG)	Horizontal Resolution	0.5° × 0.5°	0.1° × 0.1°	
	Lightning flash density rates	Lightning flash from World Wide Lightning Location Network [81] and the Lightning Mapper on GOES-R	Horizontal Resolution	50 km	10 km	

Table 1. The INCUS Science Traceability Matrix

2.1 Dynamic Atmospheric Radar (DAR)

DAR capitalizes on JPL's long history of atmospheric radar observations from CloudSat, the Airborne Second and Third Generation Precipitation Radars (APR-2/-3), and most importantly, RainCube [7-12] which has successfully completed more than 2 years of spaceborne observations before reentering the atmosphere, as well as the successful demonstration in space by other commercial endeavors of the utility of lightweight mesh deployable antennas for Ka-band [15-18]. The Dynamic Millimeter-wave Radiometer (DMR) leverages JPL's history of passive microwave observations, and is build-to-print from the TEMPEST-D radiometer [13,14], which has successfully completed more than 2 years of spaceborne observations.

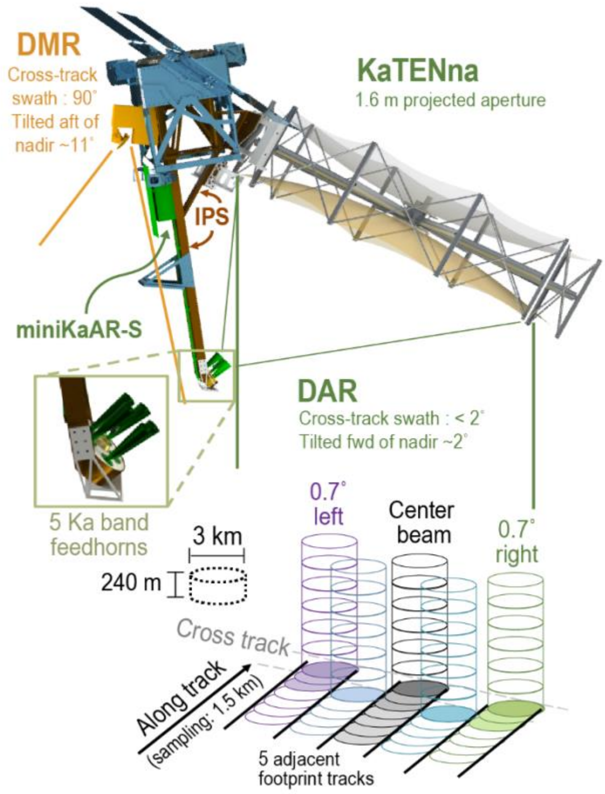

Figure 2. Notional mechanical configuration showing the IPS (brown), DAR (electronics and feedhorns in green, reflector in gold) and DMR (orange). DAR is near-nadir pointing with five beams arranged to obtain five adjacent footprint tracks, DMR is wide-swath cross-track, tilted ~13° aft with respect to DAR.

DAR is the SmallSat version of RainCube's real aperture precipitation profiling radar developed for a 6U CubeSat, which was composed of two elements: the pulsed radar miniKaAR-C (miniature Ka-band Atmospheric Radar electronics for CubeSats), and the KaRPDA (Ka-band Radar Parabolic Deployable Antenna). The former is replaced by miniKaAR-S (miniKaAR for SmallSats), which includes minor changes with respect to miniKaAR-C, and the latter is replaced by a 1.6 m antenna by TenDeg LLC, a lightweight deployable, offset-fed antenna illuminated by five standard Ka-band horns, which are activated sequentially by a front-end switch network to obtain a 5-beam cross-track swath near nadir as shown in Figure 2. DAR measures vertical profiles of radar reflectivity factor (Z_e) from precipitation – similar to the Ka-band radar on the GPM mission.

DAR key and driving requirements, main characteristics, and parameters are shown in Table 2. The horizontal resolution drives the antenna beamwidth (B_w) given the chosen platform altitude. The 1.6 m projected aperture antenna with ~0.35° B_w results in a 3.1 km horizontal footprint for an orbit altitude of 500 km. The use of 5 beams gives ~15 km cross-track swath sufficient to observe the 3-D storm structure at the meso-gamma scale and mitigate the effects of non-uniformity and horizontal advection. D-Train pointing requirements are driven by the science requirement to collocate the DAR footprints of pairs of spacecrafts to the required fractional footprint overlap.

To obtain the desired raw horizontal sampling (i.e., one profile every half footprint along track, following the findings in [19]), 25 pulses are averaged for each profile. Accounting for the range (2 bins) and along-track (2 profiles) averaging in ground processing, this results in 100 independent samples, and an expected precision of 0.41 dB.

DAR uses pulse compression to achieve high resolution with low RF peak power. The pulse characteristics (amplitude tapering and chirp bandwidth) determine the intrinsic range resolution, which equates to vertical resolution for this near-nadir-looking radar. The DAR signal and processing chains are identical to those of RainCube: the nominal chirp bandwidth is 2.5 MHz with a Hanning amplitude taper, resulting in an intrinsic range resolution of 120 m, sampled at 60 m. Range averaging in ground processing degrades it to 240 m to improve precision. Also, it is required that the resulting range sidelobes of the surface reflection do not contaminate the atmospheric return above 5 km. RainCube in-orbit measurements confirm that no range sidelobes are observed above the desired level. Simulations of the radar surface response, including antenna pattern and compressed pulse shape, were performed to verify that, at a maximum off-nadir angle of 4.3°, surface clutter is suppressed well below the noise floor at the minimum required altitude of 5 km, and they were validated with RainCube in-orbit data [20]. The resulting attitude requirements are compatible with the nominal Attitude Determination and Control System (ADCS) performance of the bus. With a receive window of 22 km and 16-bit floating point output from the data processor, the peak science data rate is 134 kbps (plus 6 kbps of state of health). This is slightly more than double that of RainCube (due to DAR's shorter integration time).

High-heritage CloudSat calibration approaches and algorithms using selected portions of the Earth's surface as calibration targets [21-30] are adopted for INCUS with important favorable factors; the Ka-band ocean surface backscatter is better characterized by state-of-the-art models with respect to W-band, and atmospheric gaseous attenuation is also significantly reduced and modeled with less uncertainty. DAR L1 data are expected to look similar to RainCube (see Figure 1) but with significantly improved horizontal resolution (3 km vs. 8 km) and sensitivity, and on 5 adjacent and contiguous curtains instead of only one.

2.2 Dynamic Millimeter wave Radiometer (DMR)

Table 3 summarizes the radiometer characteristics. DMR's footprints are 5 to 10 times wider than DAR, and they do not require to be precisely collocated to DAR because DMR's primary functions are to provide information pertaining to the environment surrounding the storms profiled by DAR and to characterize the storm anvil properties; therefore, DMR pointing requirements are 10× more relaxed than DAR's. INCUS science requires a precision of 2 K and an absolute accuracy of 5 K. The former is met by DMR with margin, the latter is met through global post-launch calibration and validation, and minimizing biases with respect to other sensors and models using well-established techniques in use by the GPM mission [31]. The DMR performance requirements are the same as TEMPEST-D whose performance was validated on-orbit.

DMR consists of four main subsystems: antenna, RF front-end, command and data handling (C&DH) electronics, and scan mechanism. The incident thermal signal enters the instrument through an open aperture and is focused by a scanning reflector onto a dual-frequency feedhorn. The two waveguide outputs of the feedhorn are connected to RF front-end millimeter-wave low noise amplifier (LNA) modules, the first operating at 87 GHz and the second with four channels from 165 to 181 GHz. At 87 GHz, the signal is amplified, filtered, and detected. From 165 to 181 GHz, the signal is amplified, multiplexed, and detected. The instrument has the capability to switch off the radiometer amplifiers when the radar transmits to mitigate the risk of damage by spurs at the radiometer operating frequencies. All four main subsystems are build-to-print copies of the ones flown in TEMPEST-D [32]. Three standard engineering auxiliary subsystems (Power, Mechanical, and Thermal) complete the DMR. The entire DMR including the antenna optics and calibration target, fits in 4U, and is packaged in a 6U CubeSat structure to maintain an identical mechanical interface.

Table 2. DAR driving requirements and parameters. RC = RainCube.

Requirement @ nadir		CBE	Margin/Risk Posture
Hor. Res.	3.5 [km]	3.1	@ 500 km altitude
Vert. Res.	250 [m]	240	Range averaging degrades to 240
Sensitivity	17 [dBZ]	8	9 dB margin
Vert. window	5 to 19 [km]	-1 to 21	>1 km of margin on each side, adjustable
Prec./ Acc.	1 / 2 [dB]	0.4/1.5	Demonstrated by CloudSat & RainCube

Parameters & Characteristics		Notes
Mass	32.5 Kg	
Power (science)	35 W @ 12V peak	
Volume	6U	Antenna separate
Transmit Power (P_t)	13 W	Same as RC
Center Freq. (f)	35.75 GHz	Same as RC
Pulse Bandwidth (B_P)	<2.5 MHz	Same as RC
Pulse Width (τ)	<200 μs	166 nom., adjust. in orbit via gnd cmd, =RC
Pulse Rep. Int.(PRI)	<2000 μs	1660 nom., adjust. in orbit via gnd cmd, =RC
Ant. Beamwidth (B_w)	0.35°	1.6 m antenna, 5 beams
Onboard Data Processing	Filtering, averaging, pulse compression	Same as RC
Operational Modes	Science, Rx Only, Initialize	Same as RC

Table 3. DMR characteristics.

Mass	3.75 kg
Volume Dimensions	10 × 20 × 20 cm^3
Operational Modes	Science/Checkout/Off
Operational Mode Timeline	Always on
Data Rate (Science)	10.3 kbps
Power (Science)	Peak: 7.0 W, Average: 6.5 W @ 12V
Thermal Control Capability	±1.5°C / orbit
Spatial Resolution	16 km (182 GHz) / 32 km (89 GHz)
Spectral Resolution	4 GHz (87 &165 GHz) 2 GHz (174, 178 & 181 GHz)
Observational Geometry Requirements	Cross track +60 / -60 deg. Cold sky view at +90 deg. for calibration
Tb Sensitivity / Accuracy	<0.9 K / 2 K
Calibration Requirements	Blackbody calibration target and cosmic microwave background
EMI/EMC Requirements	RF enable/disable functionality to turn off RF amplifiers

3 SUMMARY AND CONCLUSIONS

The INCUS mission concept aims at providing the first tropics-wide investigation of the evolution of the vertical transport of air and water by convective storms, one of the most influential, yet unmeasured atmospheric processes. Such measurements are central to NASA's Earth Science Directorate science objective to "improve the capability to predict weather and extreme weather events" [33].
The INCUS mission concept provided the strategic vision for a number of targeted technological developments spanning across all elements of cloud and precipitation radars and radiometers. Once the technological developments were successfully demonstrated in space by RainCube and TEMPEST-D, the INCUS mission concept could be proposed, with its recent selection facilitating the achievement of well documented scientific goals.

4 REFERENCES

[1] Kummerow, Christian, et al. "The Tropical Rainfall Measuring Mission (TRMM) sensor package." *Journal of Atmospheric & Oceanic Technology* 15.3 (1998).

[2] Stephens, Graeme L., et al. "CloudSat mission: Performance and early science after the first year of operation." *Journal of Geophysical Research: Atmospheres (1984–2012)* 113.D8 (2008).

[3] Tanelli, Simone, Stephen L. Durden, Eastwood Im, Kyung S. Pak, Dale G. Reinke, Philip Partain, John M. Haynes, and Roger T. Marchand. "CloudSat's cloud profiling radar after two years in orbit: Performance, calibration, and processing." *Geoscience and Remote Sensing, IEEE Transactions on* 46, no. 11 (2008): 3560-3573.

[4] Furukawa, K.; Kojima, M.; Miura, T.; Hyakusoku, Y.; Iguchi, T.; Hanado, H.; Nakagawa, K.; Okumura, M., "Proto-flight test of the Dual-frequency Precipitation Radar for the Global Precipitation Measurement," *Geoscience and Remote Sensing Symposium (IGARSS), 2011 IEEE International*, vol., no., pp.1279,1282, 24-29 July 2011. doi: 10.1109/IGARSS.2011.6049433.

[5] "Outstanding Questions in Atmospheric Composition, Chemistry, Dynamics and Radiation for the Coming Decade." Final Workshop Proceedings. 2014. https://espo.nasa.gov/home/sites/default/files/documents/SMDWorkshop_report_final.docx

[6] National Academies of Sciences, Engineering, Medicine, *Thriving on Our Changing Planet: A Decadal Strategy for Earth Observation from Space*. Washington, DC: The National Academies Press, 2018.

[7] JPL. (2018, September 25, 2018). Mini Mission RainCube is Sent into Earth Orbit. Available: https://www.jpl.nasa.gov/images/mini-mission-raincube-is-sent-into-earth-orbit

[8] E. Peral, "U.S. Patent Application No. 14/857,810, Systems and Methods for Performing Offset IQ Modulation," 2014.

[9] E. Peral, E. Im, L. Wye, S. Lee, S. Tanelli, Y. Rahmat-Samii, S. Horst, J. Hoffman, S. Yun, T. Imken, and D. Hawkins, "Radar Technologies for Earth Remote Sensing From CubeSat Platforms," *Proceedings of the IEEE,* vol. 106, pp. 404-418, 2018.

[10] E. Peral, S. Tanelli, S. Statham, S. Joshi, T. Imken, D. Price, J. Sauder, N. Chahat, and A. Williams, "RainCube: the first ever radar measurements from a CubeSat in space," *Journal of Applied Remote Sensing,* vol. 13, p. 032504, 2019. https://doi.org/10.1117/1.JRS.13.032504

[11] Available: https://www.jpl.nasa.gov/cubesat/missions/raincube.php

[12] S. Tanelli, E. Peral, E. Im, M. Sanchez-Barbetty, R. M. Beauchamp, and R. R. Monje, "RainCube and its legacy for the next generation of spaceborne cloud and precipitation radars," in *2020 IEEE Radar Conference (RadarConf20)*, 2020, pp. 1-4.

[13] S. C. Reising, T. C. Gaier, C. D. Kummerow, V. Chandrasekar, S. T. Brown, S. Padmanabhan, B. H. Lim, S. C. van den Heever, T. S. L'Ecuyer, and C. S. Ruf, "Overview of temporal experiment for storms and tropical systems (TEMPEST) CubeSat constellation mission," in *Microwave Symposium (IMS), 2015 IEEE MTT-S International*, 2015, pp. 1-4.

[14] S. C. Reising, T. C. Gaier, C. D. Kummerow, S. Padmanabhan, B. H. Lim, C. Heneghan, W. Berg, V. Chandrasekar, J. P. Olson, and S. T. Brown, "Global measurement of temporal signatures of precipitation: Development of the temporal experiment for storms and tropical systems technology demonstration mission," in *Geoscience and Remote Sensing Symposium (IGARSS), 2017 IEEE International*, 2017, pp. 5931-5933.

[15] N. Chahat, R. E. Hodges, J. Sauder, M. Thomson, E. Peral, and Y. Rahmat-Samii, "CubeSat Deployable Ka-Band Mesh Reflector Antenna Development for Earth Science Missions," *IEEE Transactions on Antennas and Propagation,* vol. 64, pp. 2083-2093, 2016.

[16] N. Chahat, T. J. Reck, C. Jung-Kubiak, T. Nguyen, R. Sauleau, and G. Chattopadhyay, "1.9-THz Multiflare Angle Horn Optimization for Space Instruments," *IEEE Transactions on Terahertz Science and Technology,* vol. 5, pp. 914-921, 2015.

[17] N. Chahat, J. Sauder, M. Mitchell, N. Beidleman, and G. Freebury, “One-Meter Deployable Mesh Reflector for Deep-Space Network Telecommunication at X-Band and Ka-Band,” *IEEE Transactions on Antennas and Propagation,* vol. 68, pp. 727-735, 2020.
[18] Y. Rahmat-Samii, V. Manohar, J. M. Kovitz, R. E. Hodges, G. Freebury, and E. Peral, “Development of Highly Constrained 1 m Ka-Band Mesh Deployable Offset Reflector Antenna for Next Generation CubeSat Radars,” *IEEE Transactions on Antennas and Propagation,* vol. 67, pp. 6254-6266, 2019.
[19] O. O. Sy, S. Tanelli, E. Peral, G.-F. Sacco, S. L. Durden, N. Chahat, S. Hristova-Veleva, B. Knosp, P. P. Li, Q. Vu, A. J. Heymsfield, and A. Bansemer, “RainCube: Scientific products from the first Radar in a CubeSat (RainCube) after two years in orbit: deconvolution, cross-validation and retrievals,” *IEEE Trans. on Geosc. and Rem. Sens.,* conditionally accepted.
[20] R. M. Beauchamp, S. Tanelli, and O. O. Sy, “Observations and Design Considerations for Spaceborne Pulse Compression Weather Radar,” *IEEE Transactions on Geoscience and Remote Sensing,* pp. 1-12, 2020.
[21] R. Meneghini and T. Kozu, “Spaceborne weather radar,” *Norwood, MA, Artech House, 1990, 208 p.,* 1990.
[22] S. Tanelli, S. L. Durden, E. Im, K. S. Pak, D. G. Reinke, P. Partain, J. M. Haynes, and R. T. Marchand, “CloudSat’s cloud profiling radar after two years in orbit: Performance, calibration, and processing,” *Geoscience and Remote Sensing, IEEE Transactions on,* vol. 46, pp. 3560-3573, 2008.
[23] A. Protat, D. Bouniol, E. O’Connor, H. Klein Baltink, J. Verlinde, and K. Widener, “CloudSat as a global radar calibrator,” *Journal of Atmospheric and Oceanic Technology,* vol. 28, pp. 445-452, 2011.
[24] A. Protat, D. Bouniol, J. Delanoë, E. O’Connor, P. May, A. Plana-Fattori, A. Hasson, U. Görsdorf, and A. Heymsfield, “Assessment of CloudSat reflectivity measurements and ice cloud properties using ground-based and airborne cloud radar observations,” *Journal of Atmospheric and Oceanic Technology,* vol. 26, pp. 1717-1741, 2009.
[25] L. Li, G. M. Heymsfield, L. Tian, and P. E. Racette, “Measurements of ocean surface backscattering using an airborne 94-GHz cloud radar-implication for calibration of airborne and spaceborne W-band radars,” *Journal of Atmospheric and Oceanic Technology,* vol. 22, pp. 1033-1045, 2005.
[26] N. Majurec, J. T. Johnson, S. Tanelli, and S. L. Durden, “Comparison of Model Predictions With Measurements of Ku-and Ka-Band Near-Nadir Normalized Radar Cross Sections of the Sea Surface From the Genesis and Rapid Intensification Processes Experiment,” *Geoscience and Remote Sensing, IEEE Transactions on,* vol. 52, pp. 5320-5332, 2014.
[27] S. Tanelli, S. L. Durden, and E. Im, “Simultaneous measurements of Ku-and Ka-band sea surface cross sections by an airborne radar,” *Geoscience and Remote Sensing Letters, IEEE,* vol. 3, pp. 359-363, 2006.
[28] R. Meneghini, H. Kim, L. Liao, J. A. Jones, and J. M. Kwiatkowski, “An initial assessment of the surface reference technique applied to data from the dual-frequency precipitation radar (DPR) on the GPM satellite,” *Journal of Atmospheric and Oceanic Technology,* vol. 32, pp. 2281-2296, 2015.
[29] D. Josset, S. Tanelli, Y. Hu, J. Pelon, and P. Zhai, “Analysis of water vapor correction for Cloudsat W-band radar,” *Geoscience and Remote Sensing, IEEE Transactions on,* vol. 51, pp. 3812-3825, 2013.
[30] H. Liebe, G. Hufford, and M. Cotton, “Propagation modeling of moist air and suspended water/ice particles at frequencies below 1000 GHz,” in *In AGARD, Atmospheric Propagation Effects Through Natural and Man-Made Obscurants for Visible to MM-Wave Radiation 11 p (SEE N94-30495 08-32)*, 1993.
[31] W. Berg, S. Bilanow, R. Chen, S. Datta, D. Draper, H. Ebrahimi, S. Farrar, W. L. Jones, R. Kroodsma, and D. McKague, “Intercalibration of the GPM microwave radiometer constellation,” *Journal of Atmospheric and Oceanic Technology,* vol. 33, pp. 2639-2654, 2016.

[32] S. Padmanabhan, T. C. Gaier, A. B. Tanner, S. T. Brown, B. H. Lim, S. C. Reising, R. Stachnik, R. Bendig, and R. Cofield, "TEMPEST-D Radiometer: Instrument Description and Prelaunch Calibration," *IEEE Transactions on Geoscience and Remote Sensing,* pp. 1-14, 2020.

[33] NASA. (2014). *2014 Science Plan*. Available: https://smd-prod.s3.amazonaws.com/science-red/s3fs-public/atoms/files/2014_Science_Plan_PDF_Update_508_TAGGED_1.pdf

.